Journal of Mathematical Imaging and Vision 18: 129–143, 2003

Numerical Schemes of Shock Filter Models for Image Enhancement and Restoration

L. REMAKI AND M. CHERIET
Laboratory for Imagery, Vision and Artificial Intelligence, École de technologie supérieure, 1100 Notre-Dame West, Montreal, Quebec, Canada H3C 1K3
remaki@livia.etsmtl.ca
cheriet@gpa.etsmtl.ca

Abstract. Considerable interest has recently been given to signal processing models based on partial differential equations. Successively improved models based on hyperbolic partial differential equation types are proposed in the literature. These models yield interesting results; however, it would be of great interest to generalize them in order to increase their efficiency. In this paper, we propose a generalized shock filter model for one-dimensional signal restoration. After justifying the existence and uniqueness of the solutions in an adequate vector space, we propose an effective numerical scheme to discretize the proposed model, and derive a two-dimensional numerical scheme directly from the one-dimensional model following a space-split strategy. We then prove a stability result for both schemes. We conclude our study by providing high-quality experimental results for one- and two-dimensional signal enhancement and restoration, and showing the influence the shock speed control has on processing time.

Keywords: numerical schemes, shock filters, partial differential equations, PDEs, stability, signal enhancement and restoration

1. Introduction

Significant interest in the mathematical formulation of problems related to the field of signal processing has been observed over the past decade. The majority of these techniques require the use of partial differential equations (PDEs). In several cases, the PDE-based approaches guarantee the existence and uniqueness of the targeted solution, and provide powerful numerical schemes. Image enhancement and restoration, the focus of this paper, is one of the fields that makes extensive use of PDEs. Successive theoretically and practically improved models (isotropic and anisotropic cases) are proposed in the literature: examples include Koendrink [6], Perona and Malik [9], Osher and Rudin [8], Alvarez et al. [1], and Alvarez and Mazorra [2].

These models yield satisfactory results; however, it would be of great interest to generalize them by introducing new parameters that increase the model efficiency and exercise tighter control over the enhancement and restoration process, as well as adaptation to specific situations. The challenge in doing so is to keep the obtained model well-posed (existence and uniqueness of the solutions). This is clearly no easy task, since the coefficients used in the model are often discontinuous functions, and the processed signals are also discontinuous. Consequently, their space derivatives are Dirac functions. We are then confronted with a product of distributions, which is nonsensical according to the classical theory of distributions (see [4] for the Schwartz theorem). However, within the framework of generalized functions introduced by Colombeau [4], the product of distribution is coherent without contradicting the Schwartz theorem. This is made possible by the introduction of the association notion (referred by "$\approx$"), which is a generalization of the equality notion (refer to [4] for a detailed study of this theory). In this paper, we propose a generalized model in the one-dimensional case of the model proposed by Osher and Rudin [8] with some added modifications that allow us to obtain a model fitting with that studied in [10]. This in turn guarantees the well-posedness of the model

within the framework of generalized function algebra. We then propose a stable explicit numerical scheme to discretize the proposed model. Using a space-split strategy, we derive a stable explicit numerical scheme for image enhancement and restoration. By proceeding in this manner, a two-dimensional model formulation is not required. Only the one-dimensional model is considered here, over which we generally have greater control. The proposed numerical schemes are the focus of this paper; their stability, in a sense that will be defined, is proved in both cases. Tests proving the schemes' performance when restoring signals in one and two dimensions are performed. We also show the effectiveness of the parameters introduced in the model with regards to processing time through targeted tests.

2. Overview of Previous Works

In [8], Osher and Rudin propose a shock filter model that develops shocks in the laplacian zero-crossing position. Unfortunately, the influence of noise causes this model to produce a great quantity of spurious shocks. In order to avoid them, Alvarez and Mazorra [2] have proposed the improved hyperbolic partial differential model:

$$u_t + F(G_\sigma * u_{xx}, G_\sigma * u_x)u_x = 0 \text{ in } \Re \times \Re^+$$

where $G_\sigma(\cdot)$ is a smoothing kernel and F satisfies $srF(s, r) \geq 0$. Alvarez and Mazorra developed an interesting recursive, unconditional, stable implicit scheme. This model yields satisfactory results, as shown in [2]. However, to give a larger scope of application to the models derived from a shock filter theory, we believe it necessary to maintain heightened control of the created shocks' velocity. In the models cited previously, the velocity represented by the function $F(G_\sigma * u_{xx}, G_\sigma * u_x)$ controls the position where the model develops shocks, but not the intensity of the velocity according to the features of the signal, or what we target in the enhancement and restoration process. In the following section, we propose a model which takes these issues into account. The challenge is to preserve the well-posedness of the obtained model. An interpretation of the model within an adequate vector space guarantees the existence and uniqueness of solution.

Before developing the proposed model, we shall give a brief overview of the generalized function space, which is the framework in which this model is considered. Introduced by Colombeau [3, 4], this space was chosen because it contains the distribution space. Moreover, this space is an algebra, which allows the product of distributions to make sense. Since we are dealing with functions representing images, which are discontinuous functions, a product of distribution occurs in PDE-based models which makes no sense within the classical space of distribution.

3. Overview of the Generalized Function Space

The following is an overview of the generalized function algebra, also known as the Colombeau algebra. For details about this theory, see [3].

Definition 1. If $q = 0, 1, 2, \ldots$ we set $A_q = \{\varphi \in D(\Re^n)$ such that $\int \varphi\, dx = 1$ and $\int x^j \varphi\, dx = 0$ if $1 \trianglelefteq j \trianglelefteq q\}$.

We define by $E(\Omega)$ the set of functions R such that:

$$R : A_1 \times \Omega \to \Re$$
$$(\Phi, x) \to R(\Phi, x)$$

where R is a C^∞ function on x for each fixed Φ.

Property 1. *The set $E(\Omega)$ is an algebra and $C^\infty(\Omega)$ is a sub-algebra of $E(\Omega)$.*

Definition 2. We define by $E_M(\Omega)$ the sub-algebra of $E(\Omega)$ functions that have a moderate increase. This means that:

$$E_M(\Omega) = \left\{ \begin{array}{l} R\text{: such that for each compact set } K, \\ \quad \text{for each derivative of order } p, \text{ there} \\ \quad \text{exists an integer } N \text{ such that if } \Phi \in \\ \quad A_N, \text{ then there exists } \eta > 0, C > 0 \\ \quad \text{such that: } \mathrm{Sup}_{x \in K} |R_\varepsilon^{(p)}(\Phi, x)| \leq \\ \quad C(\frac{1}{\varepsilon})_N \text{ with } 0 < \varepsilon < \eta < 1 \end{array} \right\}$$

where $R_\varepsilon(\Phi, x) = R(\Phi_\varepsilon, x)$ and $\Phi_\varepsilon(\lambda) = \frac{1}{\varepsilon^n}\Phi(\frac{\lambda}{\varepsilon})$.

Definition 3. We define the set $I(\Omega)$ as:

$$I(\Omega) = \left\{ \begin{array}{l} R \in E_M(\Omega) \text{ such that for any compact} \\ \quad \text{set } K \text{ of } \Omega, \text{ for any derivative of order} \\ \quad p, \text{ there exists an integer } N \text{ such that} \\ \quad \text{for each function } \Phi \in A_N, \text{ there exists} \\ \quad \text{a cons tan } t, C > 0 \text{ and } \eta > 0, \text{ such} \\ \quad \text{that for each sufficiently } l \arg eq \text{ we} \\ \quad \text{have: } \mathrm{Sup}_{x \in K} |R_\varepsilon^p(\Phi, x)| \leq C(\frac{1}{\varepsilon})^{q-N} \\ \quad \text{with } 0 < \varepsilon < 0. \end{array} \right\}$$

Property 2. *The set $I(\Omega)$ is a vectorial subspace and an ideal of $E_M(\Omega)$.*

We are now able to define the generalized function algebra.

Definition 4. The C^∞ generalized function algebra $G(\Omega)$ is defined as the quotient:

$$G(\Omega) = \frac{E_M(\Omega)}{I(\Omega)}$$

The above definition of the generalized function algebra is rather abstract and, practically-speaking, how to handle the elements of $G(\Omega)$ is not evident. Thus, we define a simplified space of the generalized function algebra (G_s) without a canonical inclusion of the distributions. Refer to Chapter 8 of [3] regarding this immediate simplification.

If Ω is any open set in R^n, we define a space of "simplified global generalized functions" as follows. The reservoir of representatives is:

$$E_s(\Omega) = \left\{ \begin{array}{l} \text{all maps } \Re \in C^\infty(]0,1] \times \Omega,\ R), \text{ such} \\ \quad \text{that, } \forall D \text{ (partial } x \text{ derivative, includ-} \\ \quad \text{ing the identity) } \exists N \in \mathbb{N},\ c > 0, \\ \quad \text{such that: } \forall x \in \Omega,\ |(DR)(\varepsilon, x)| \leq \frac{c}{\varepsilon^N} \end{array} \right\}$$

and the ideal of $E_s(\Omega)$ is:

$$\begin{aligned} N_s(\Omega) = \{ & R \in C^\infty(\Omega),\ \text{such that: } \forall D, \forall q \in \mathbb{N} \\ & \exists c_q > 0,\ \text{such that: } \forall x \in \Omega, \\ & |(DR)(\varepsilon, x)| \leq c_q \varepsilon^q \}. \end{aligned}$$

Then the space $G_{s,g}(\Omega)$ of the simplified global generalized functions on Ω is the quotient algebra $G_{s,g}(\Omega) = \frac{E_s(\Omega)}{N_s(\Omega)}$. The term "global" is employed in this instance because the above bounds hold globally on Ω, and not only on compact subsets of Ω, as in [3].

3.1. The Association Concept

We say that $G_1, G_2 \in G_s(\Omega)$ are associated (we write $G_1 \approx G_2$), if and only if, for any Ψ in $D(\Omega)$, we have:

$$\int_\Omega [R_1(\varepsilon, x) - R_2(\varepsilon, x)\Psi(x)]\, dx \to 0 \text{ when } \varepsilon \to 0$$

where $R_1 \in E_s$ is a representative of G_1 and $R_2 \in E_s$ is a representative of G_2.

The association could be viewed as a weak generalization of the equality concept. Consequently, when dealing with PDE equations, the equality is replaced by the association unless we are certain about the equality.

3.2. The Product of Generalized Functions

The product of two generalized functions is defined naturally by the class of the product of its representatives (by replacing the equality with the association concept) i.e., if $G_1, G_2 \in G_s(\Omega)$ and R_1, R_2 are their respective representatives, then $G_1 \cdot G_2 \approx$ Class $\{R_1 \cdot R_2\}$. A non-linear regular function of generalized functions is defined in more general terms in [4].

Now we will examine which classical functions or distributions can be represented by generalized functions.

3.2.1. Inclusions. Let f be a function in the space $D_{L^\infty}(\Omega)$, i.e., f is a C^∞ function on Ω, globally bounded on Ω as well as its derivatives; then with f, associate $R(\varepsilon, x) = f(x)$. This gives the inclusion $D_{L^\infty}(\Omega) \subset G_s(\Omega)$. Let f be a function in the space $L^\infty(\mathbb{R}^n)$; then with f, associate $R(\varepsilon, x) = f * \rho_\varepsilon(x)$ with a chosen $\rho \in D(\mathbb{R}^n)$, $\int \rho(\lambda)\, d\lambda = 1$ and $\rho_\varepsilon(\lambda) = \frac{1}{\varepsilon^n}\rho(\frac{\lambda}{\varepsilon})$. For any given mollifier ρ, this gives an inclusion $L^\infty(\mathbb{R}^n) \subset G_s(\mathbb{R}^n)$. More generally, let T be a distribution in $D'_{L^\infty}(\mathbb{R}^n)$, i.e., T is a finite sum of the derivatives of functions in $L^\infty(\mathbb{R}^n)$. With T, associate $R(\varepsilon, x) = (T * \rho_\varepsilon)(x)$ as above. Therefore, for a given ρ, this provides an inclusion of $D'_{L^\infty}(\mathbb{R}^n)$ in $G_s(\mathbb{R}^n)$. Similarly, there is an inclusion of $E'(\Omega)$—the space of all distributions with compact support—in $G_s(\Omega)$. All the above inclusions become canonical, i.e. the arbitrariness in the choice of a mollifier ρ disappears if one works in the space $G(\Omega)$ of "non-simplified" generalized functions, exactly as in chapter 8 of [6], whose definition is slightly more complex.

Proposition. *Let $T \in D'(\Omega)$. Then there exists $g \in G_{s,g}(\Omega)$ associated with T. We write $g \approx T$ and say that T is the "macroscopic aspect" of g. (The proof is given in* [3, 4].)

3.2.2. Derivatives of Generalized Functions. A derivative of a generalized function (∂g) is naturally defined by the class of equivalence of a given representative. That is, if $R(\varepsilon, x)$ is a representative of g, $\partial g =$ Class $\partial R(\varepsilon, x)$.

3.3. Regularized Derivatives

The concept of regularized derivatives ($\bar{\partial}$) constitutes the basic ingredient ensuring existence and uniqueness results in many situations. The properties of these derivatives are discussed in [7, 8]; we recall, for instance, that if g is a generalized function then $\bar{\partial} g$ and ∂g are associated in $G_{s,g}$. We shall now give the definition of $\bar{\partial}$:

If $R(\varepsilon, x)$ is a representative of a generalized function g, if ∂ is a partial x-derivative, if $\rho : \Re^n \to \Re$ with $\int \rho(\mu)\, d\mu = 1$ ($\rho \in D(\Re^n)$, or ρ step function) is a "mollifier" and if $h : \varepsilon \to h(\varepsilon)$ is a scaling function ($h : [0,1] \to [0,1]$ and $h(\varepsilon) \to 0$ when $\varepsilon \to 0$), then the mollified derivative $\tilde{\partial}^h g$ is the class of $(\partial R(\varepsilon, \cdot) * \rho_{h(\varepsilon)})(x)$.

4. Our One-Dimensional Shock Filter Model

In this section, we present a description of our generalized one-dimensional model. In the following sections, a justification of the existence and uniqueness solution within the framework of the generalized function algebra is given. An explicit numerical scheme is then proposed, and a two-dimensional numerical scheme for image restoration and enhancement is derived proving the stability of both schemes (one and two dimensions).

As a model, we propose the following one-dimensional quasi-linear equation with discontinuous coefficients:

$$u_t + a(x) F\left(u^0_{xx}, u^0_x\right) \partial_x f(u(x,t)) = 0 \text{ in } \Re \times \Re^+ \quad (1)$$

where u^0 is the original signal, a is a bounded and measurable discontinuous function, and F and f are regular (smooth) functions. The convolution of F arguments is omitted from this model. The smoothing operation is inherent to the model when the problem is considered via the generalized function theory. The function F plays the same role as in the previous models. The derivatives in its arguments are taken on the original image; as a result, this function is only computed once (at the beginning of the process). Furthermore, we believe that by doing so, we minimize the impact of the problem of locating the edges, which may move during the process. Introducing the coefficients $a(x)$ and f controls the shock velocity according to the characteristics of the original signal and/or what is targeted. In Section 10, we demonstrate through tests how controlling the propagation speed (velocity) can accelerate the restoration process appreciably. According to the classical theory of distributions, considering the derivatives of the original signal (which is a discontinuous function) in the model makes the problem ill-posed. However, interpreting the equation within the framework of generalized functions G (using the regularized derivatives concept [4, 7, 10]) provides an existence and uniqueness result, thereby rendering the problem well-posed. An interpretation of a general *Cauchy* problem within G consisting of a regularization (smoothing) of space derivatives is proposed in [4, 7].

5. Well-Posedness of the Model (Existence and Uniqueness Result)

Let us recall the following existence and uniqueness result proved in [10]:

Theorem. *Let u^0 belong to $L^\infty(\Re)$ and f a C^∞ bounded function and B a generalized function with a macroscopic aspect T belonging to $L^\infty(\Re)$. Let U^0 be the image in $G_{\varepsilon,g}(\Re)$ of u^0 by the embedding of $L^\infty(\Re)$ into $G_{\varepsilon,g}(\Re)$ (obtained by a regularization process). We assume that the scale function $h(\varepsilon) \to 0$ is sufficiently slow. Thus, the following equation has a unique solution U in $G_{\varepsilon,g}(\Re^+ \times \Re)$:*

$$U_t + B(x)\bar{\partial}_x f(U(x)) = 0 \text{ in } \Re \times \Re^+$$
$$U(x,0) = U^0$$

where $\bar{\partial}$ is the regularized operator (defined above), and U is the class of equivalence of a representative u^ε which is a solution of the following equation:

- *If $b^\varepsilon(\cdot) f'(\cdot) > 0$ we have*:

$$\partial_t u^\varepsilon(x,t) = -b^\varepsilon(x) \times f'(u^\varepsilon(x,t)) \times \left(\frac{u^\varepsilon(x,t) - u^\varepsilon(x-h,t)}{h}\right) \quad (2)$$
$$u^\varepsilon(x,0) = u^{0,\varepsilon} (\text{with } u^{0,\varepsilon} \text{ a } C^\infty \text{ function and } u^0 = \text{Class of } u^{0,\varepsilon})$$

- *If $b^\varepsilon(\cdot) f'(\cdot) < 0$ we have*:

$$\partial_t u^\varepsilon(x,t) = -b^\varepsilon(x) \times f'(u^\varepsilon(x,t)) \times \left(\frac{u^\varepsilon(x+h,t) - u^\varepsilon(x,t)}{h}\right) \quad (3)$$
$$u^\varepsilon(x,0) = u^{0,\varepsilon} (\text{with } u^{0,\varepsilon} \text{ a } C^\infty \text{ function and } u^0 = \text{Class of } u^{0,\varepsilon})$$

- *If $a(\cdot)^{\varepsilon} f'(\cdot)$ has an unknown sign*

$$\begin{aligned}\partial_t v^{\varepsilon}(y,t) &= -(b^{\varepsilon}(y) \times f'(v^{\varepsilon}(y,t)) - C) \\ &\quad \times \left(\frac{v^{\varepsilon}(y+h,t) - v^{\varepsilon}(y,t)}{h}\right) \quad (4) \\ v(y) &= u(y - Ct) \\ C \text{ a constant such that } C &< \mathrm{Inf}(b^{\varepsilon}(\cdot)\, f''(\cdot)) \\ y = x + Ct &\text{ a Gallelian change of variables.}\end{aligned}$$

Where $u^{0,\varepsilon} = u^0 * (\frac{1}{h_1(\varepsilon)}\rho(\frac{x}{h_1(\varepsilon)}))$ and U^0 is the equivalent class of $u^{0,\varepsilon}$. b^{ε} is a representative of B. ρ is a C^{∞} smoothing function (mollifier) supported on the unit ball. The $*$ operator is the convolution product. The scale variables, $h_1(\varepsilon)$ and $h(\varepsilon)$, are functions which tend conveniently to 0, and are chosen so that the previous function and their derivatives are moderate functions.

Now consider u^0 as a generalized function and u^0_{xx} and u^0_x its generalized first and second derivatives. Let $u^{0,\varepsilon}_{xx}$ and $u^{0,\varepsilon}_x$ be their respective representatives as defined above. Furthermore, let $a^{\varepsilon}(\cdot)$ be the representative of $a(\cdot)$ obtained by a regularized process. Since $F(\cdot,\cdot)$ and $a(\cdot)$ are bounded functions, the sequence (an extracted subsequence) $a^{\varepsilon}(x)\ F(u^{0,\varepsilon}_{xx}, u^{0,\varepsilon}_x)$ converges for the weak * topology to a function $T(x)$ belonging to $L^{\infty}(\Re)$. This means that the generalized function $B(x) \approx a(x)F(u^0_{xx}, u^0_x)$ (the class of equivalence of $b^{\varepsilon}(x) = a^{\varepsilon}(x)F(u^{0,\varepsilon}_{xx}, u^{0,\varepsilon}_x)$) admits T as a macroscopic aspect. Thus, the existence and uniqueness theorem holds for Eq. (1) interpreted within the framework of generalized functions.

In [10], the following maximum principle result is proved.

Theorem (*Maximum Principle*). *If u^{ε} is a solution of* (2) *or* (3), *and $u^{0,\varepsilon}$ vanishes when x is close to infinity, we then have*:

$$\mathrm{Inf}\, u^{0,\varepsilon}(x) \le u^{\varepsilon}(x,t) \le \mathrm{Sup}\, u^{0,\varepsilon}(x) \text{ on } \Re \times [0,T]$$

As a consequence of this result, the change of the restored image depends continuously on the change of the initial image in the $L^{\infty}(\Re)$ norm.

6. Numerical Scheme for One-Dimensional Signals

We proceed with a local resolution of Eq. (1) in G. We then use the formulation given above for representatives, depending on the propagation velocity's sign. Let us now set the following classical notations:

$$u_i^{\varepsilon,n} = u^{\varepsilon}(x_i = i\,\Delta x, t_n = n\Delta t),$$

Δx and Δt are the spatial and time mesh sizes respectively,

$$\begin{aligned}\partial_t u^{\varepsilon}(t_n, x_i) &= \frac{u_i^{\varepsilon,n+1} - u_i^{\varepsilon,n}}{\Delta t},\ \partial_x u^{\varepsilon,0}(t_n, x_i) \\ &= \frac{u_{i+1}^{\varepsilon,0} - u_i^{\varepsilon,0}}{\Delta h}\end{aligned}$$

and

$$\partial_{xx} u^{\varepsilon,0}(t_n, x_i) = \frac{u_{i+1}^{\varepsilon,0} - 2u_i^{\varepsilon,0} + u_{i-1}^{\varepsilon,0}}{\Delta h}.$$

For each couple (x_i, t_n), the approximation $u_i^{\varepsilon,n}$ of $u^{\varepsilon}(x_i, t_n)$ is the discrete solution of (2) if $a(x_i)$ $F(u^0_{xx}(x_i), u^0_x(x_i))f'(u^{\varepsilon}(x_i, t_{n-1})) > 0$, and the discrete solution of (3) if $a(x_i)F(\Delta u^0(x_i))f'(u^{\varepsilon}(x_i, t_{n-1})) < 0$. This leads to the following numerical scheme.

By setting $h = \Delta x$ and $r = \frac{\Delta t}{\Delta x}$, we obtain:

$$\begin{aligned}&u_i^{\varepsilon,n+1} \\ &= u_i^{\varepsilon,n} - r\mathrm{Max}\left[0, a_i F\left(\begin{matrix}\frac{u_{i+1}^{\varepsilon,0} - 2u_i^{\varepsilon,0} + u_{i-1}^{\varepsilon,0}}{h^2}, \\ \frac{u_{i+1}^{\varepsilon,0} - u_i^{\varepsilon,0}}{h}\end{matrix}\right) f'\left(u_i^{\varepsilon,n}\right)\right] \\ &\quad \times \left(u_i^{\varepsilon,n} - u_{i-1}^{\varepsilon,n}\right) \\ &\quad - r\mathrm{Min}\left[0, a_i F\left(\begin{matrix}\frac{u_{i+1}^{\varepsilon,0} - 2u_i^{\varepsilon,0} + u_{i-1}^{\varepsilon,0}}{h^2}, \\ \frac{u_{i+1}^{\varepsilon,0} - u_i^{\varepsilon,0}}{h}\end{matrix}\right) f'\left(u_i^{\varepsilon,n}\right)\right] \\ &\quad \times \left(u_{i+1}^{\varepsilon,n} - u_i^{\varepsilon,n}\right) \quad (5) \\ &u_i^{\varepsilon,0} = u^{\varepsilon,0}(ih).\end{aligned}$$

7. Numerical Scheme for Images

We propose a two-directional numerical scheme based on splitting in both the x-direction and y-direction, with the one-dimensional scheme then used in each direction. Set $u(x, y, t)$ as a generated image at time t and $u(x, y, 0)$ as the original image.

7.1. *x-Direction Splitting*

In the x-direction, we consider the equation:

$$u_t + a_1 F_1\left(u^0_{xx}(x,y), u^0_x(x,y)\right)\partial_x f_1(u(x,y,t) = 0$$

We then compute the approximation of u at the point $(x_i, y_j, (n + \frac{1}{2})\Delta t)$, where $x_i = i\,\Delta x$ and $x_j = j\,\Delta y$.

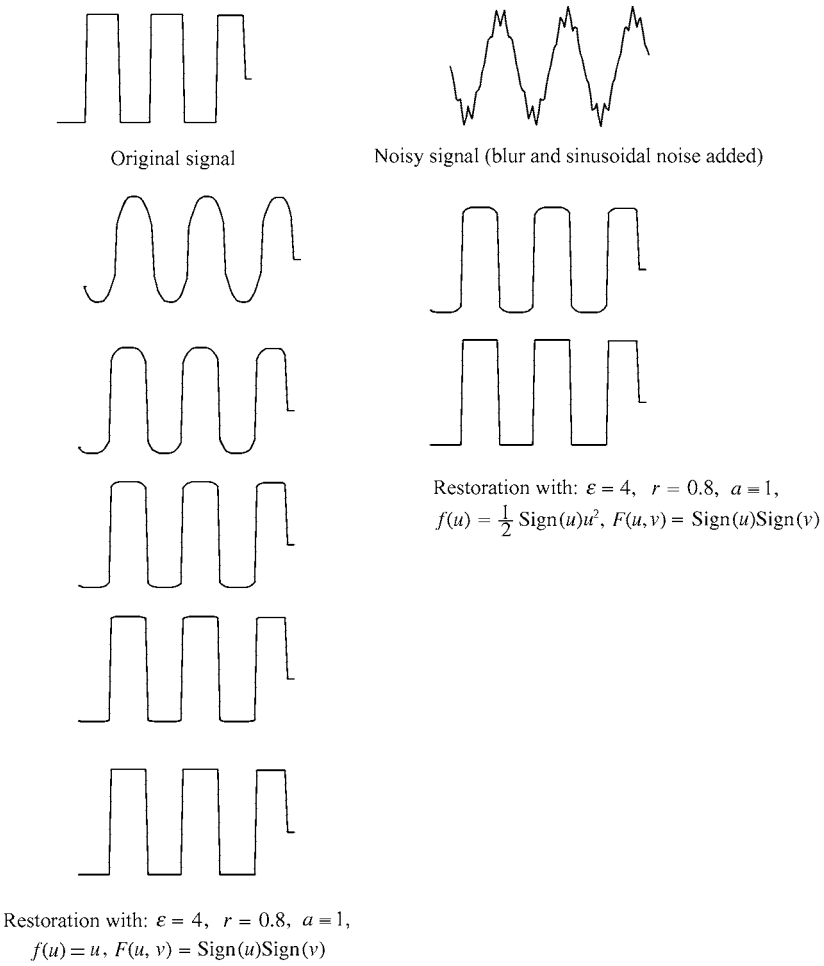

Figure 1. Enhancement and restoration of a noisy gate signal, with different values of the speed control function f. The restored signals are displayed every second iterations for both experiments. We can see that the signal is perfectly restored for both choices. The same results obtained after five steps with less speed control ($f(u) = u$) are obtained after only two steps when the speed control is heightened ($f(u) = \frac{1}{2}\,\mathrm{Sign}(u)u^2$).

Using numerical scheme (4) and by taking the notation:

$$u^{\varepsilon}\left(x_i, y_j, \left(n + \frac{1}{2}\Delta t\right)\right) = u_{i,j}^{\varepsilon,n+\frac{1}{2}},$$

we obtain:

$$u_{i,j}^{\varepsilon,n+\frac{1}{2}} = u_{i,j}^{\varepsilon,n} - \frac{1}{2}r_1\,\mathrm{Max}\left[0, a_{i,j}^1 F_1 \times \begin{pmatrix} \frac{u_{i+1,j}^{\varepsilon,0} - 2u_{i,j}^{\varepsilon,0} + u_{i-1,j}^{\varepsilon,0}}{h_1^2}, \\ \frac{u_{i+1,j}^{\varepsilon,0} - u_{i,j}^{\varepsilon,0}}{h_1} \end{pmatrix} f'\left(u_{i,j}^{\varepsilon,n}\right)\right] \times \left(u_{i,j}^{\varepsilon,n} - u_{i-1,j}^{\varepsilon,n}\right)$$

$$- \frac{1}{2}r_1\,\mathrm{Min}\left[0, a_{i,j}^1 F_1 \begin{pmatrix} \frac{u_{i+1,j}^{\varepsilon,0} - 2u_{i,j}^{\varepsilon,0} + u_{i-1,j}^{\varepsilon,0}}{h_1^2}, \\ \frac{u_{i+1,j}^{\varepsilon,0} - u_{i,j}^{\varepsilon,0}}{h_1} \end{pmatrix} \times f'\left(u_{i,j}^{\varepsilon,n}\right)\right] \left(u_{i+1,j}^{\varepsilon,n} - u_{i,j}^{\varepsilon,n}\right) \tag{6}$$

$$u_i^{\varepsilon,0} = u^{\varepsilon,0}(ih_1, jh_2).$$

7.2. *y-Direction Splitting*

In the y-direction, we consider the equation:

$$u_t + a_2 F_2\left(u_{yy}^0, u_y^0\right)\partial_y f_2(u) = 0$$

we compute the approximation of u at the point $(x_i, y_j, n)\Delta t)$.

$$u_{i,j}^{\varepsilon,n+1} = u_{i,j}^{\varepsilon,n+\frac{1}{2}} - \frac{1}{2} r_2 \operatorname{Max}\left[0, a_{i,j}^2 F_2 \left(\begin{array}{c} \frac{u_{i,j+1}^{\varepsilon,0} - 2u_{i,j}^{\varepsilon,0} + u_{i,j-1}^{\varepsilon,0}}{h_2^2}, \\ \frac{u_{i,j+1}^{\varepsilon,0} - u_{i,j}^{\varepsilon,0}}{h_2} \end{array}\right) f'\left(u_{i,j}^{\varepsilon,n+\frac{1}{2}}\right)\right] \times \left(u_{i,j}^{\varepsilon,n+\frac{1}{2}} - u_{i,j-1}^{\varepsilon,n+\frac{1}{2}}\right)$$

$$- \frac{1}{2} r_2 \operatorname{Min}\left[0, a_{i,j}^2 F_2 \left(\begin{array}{c} \frac{u_{i,j+1}^{\varepsilon,0} - 2u_{i,j}^{\varepsilon,0} + u_{i,j-1}^{\varepsilon,0}}{h_2^2}, \\ \frac{u_{i,j+1}^{\varepsilon,0} - u_{i,j}^{\varepsilon,0}}{h_2} \end{array}\right) \times f'\left(u_{i,j}^{\varepsilon,n+\frac{1}{2}}\right)\right] \left(u_{i,j+1}^{\varepsilon,n+\frac{1}{2}} - u_{i,j}^{\varepsilon,n+\frac{1}{2}}\right) \tag{7}$$

Here $h_1 = \Delta x$ and $h_2 = \Delta y$.

8. Stability Result

One of the key sought-after properties of numerical schemes is stability. This property helps to prevent the

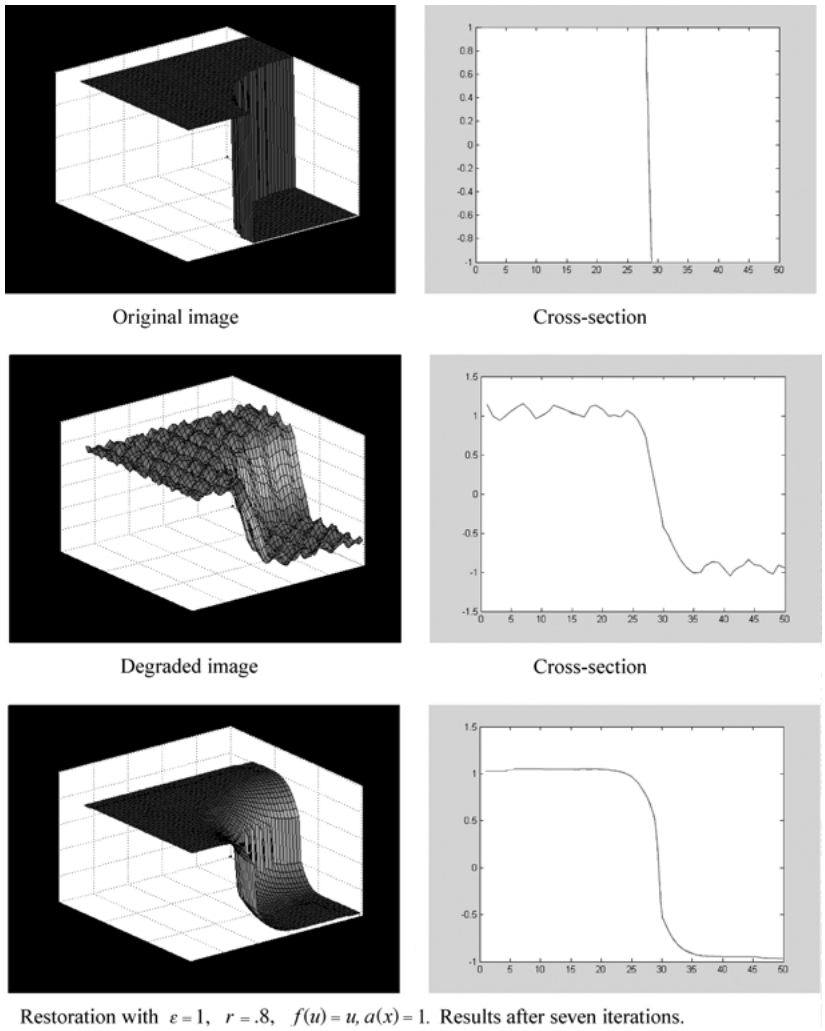

Figure 2. Curved shock test case. Convergence speed using different values of the coefficient $a(x)$.

(*Continued on next page.*)

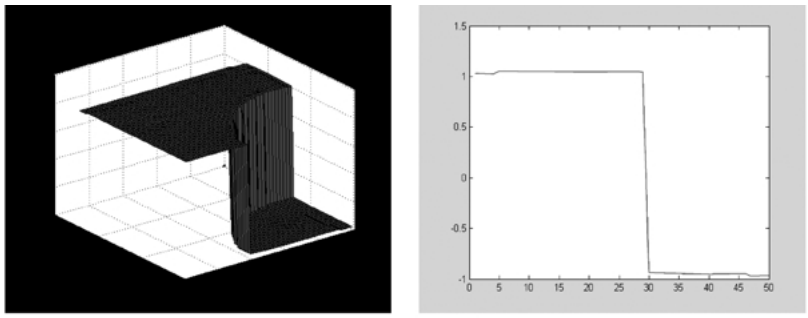

Restoration with $\varepsilon = 1$, $r = .8$, $f(u) = u$, $a(x) = 1 + (1 - u^0)(1 + u^0)$. Results after seven iterations.

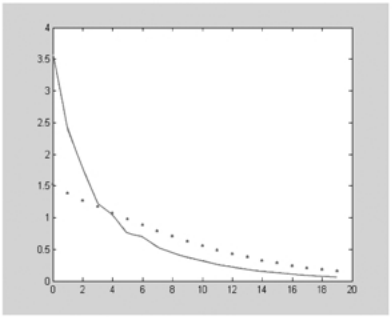

Residual curves according to the number of iterations: $a(x) = 1 + (1 - u^0)(1 + u^0)$ (continuous curve) and $a(x) = 1$ (dotted curve).

Figure 2. (*Continued*).

numerical oscillations that can appear during the recursive process, in addition to keeping the numerical scheme from exploding, then naturally diverging. We will now claim the following proposition:

Proposition. *Assume that* a, F, f', a_1, a_2, F_1, f_1', F_2 *and* f_2' *belong in* $L^\infty(\Re)$ *and* u^0 *belongs in* $BV(\Re) \cap L^\infty(\Re)$ (*see* [5] *for definitions*). *Under the CFL conditions* $r|aFf'| < \frac{1}{2}$, $r_1|a_1F_1f_1'| < \frac{1}{2}$ *and* $r_2|a_2F_2f_2'| < \frac{1}{2}$, *both numerical schemes are stable for the* L^∞*-norm and total variation in space and time.*

For the one-dimensional case:

(i) $|u_i^{\varepsilon,n}| \le \|u_0\|_{L^\infty(\Re)}, \forall i \in Z, \forall n \in \mathbb{N}$
(ii) $\sum_{i\in Z} |u_{i+1}^{\varepsilon,n} - u_i^{\varepsilon,n}| \le TV(u_0), \forall n \in \mathbb{N}$
(iii) $\sum_{i\in Z} |u_i^{\varepsilon,n+1} - u_i^{\varepsilon,n}| \le TV(u_0), \forall n \in \mathbb{N}$

For the two-dimensional case:

(i) $|u_{i,j}^{\varepsilon,n}| \le \|u_0\|_{L^\infty(\Re)}, \forall i, j \in Z, \forall n \in \mathbb{N}$
(ii) $\sum_{i,j\in Z} |u_{i+1,j}^{\varepsilon,n} - u_{i,j}^{\varepsilon,n}| + |u_{i,j+1}^{\varepsilon,n} - u_{i,j}^{\varepsilon,n}| \le TV(u_0)$, $\forall n \in \mathbb{N}$
(iii) $\sum_{i,j\in Z} |u_{i,j}^{\varepsilon,n+1} - u_{i,j}^{\varepsilon,n}| \le TV(u_0), \forall n \in \mathbb{N}$

Proof: (see Appendix). □

9. Comments on the Convergence of the $u^{\varepsilon,n}$ Sequence

A question that naturally comes to mind is the relationship of the $u^{\varepsilon,n}$ sequence with the model's generalized solution. In other words, in which sense does the sequence converge to the generalized solution? Note first that through the maximum principle, the representative u^ε (or a subsequence of u^ε) converges to a function u in $L^\infty(\Re)$ for the weak topology. u is then the macroscopic aspect of the generalized solution (which is not necessarily a solution of the equation). The $u^{\varepsilon,n}$ sequence converges to u. This claim will not be proved here, however, because it is not the focus of this paper.

10. Experimental Results

This section presents experiments concerning signal enhancement and restoration. In all of these experiments, we used a kernel with compact support (KCS) with ε as the scale parameter (see [11]) as a mollifier to smooth the original signal in order to

obtain $u^{\varepsilon,0}$. The KCS (see formula below) was selected in order to respect the theoretical development where a kernel with compact support was necessary for the regularization process, although a Gaussian kernel was also an option since, in practice, we truncate the Gaussian and its support becomes finite.

$$\rho_\varepsilon(x) = \begin{cases} \dfrac{1}{\varepsilon} e^{\left(\frac{3\varepsilon^2}{x^2-\varepsilon^2}+3\right)} & \text{if } x^2 < \varepsilon^2 \\ 0 & \text{elsewhere} \end{cases}$$

10.1. One-Dimensional Case

In Fig. 1, a blurred gate signal with added sinusoidal noise is restored following two experiments: in the first, we set $f(u) = u$ to obtain the first restoration, and in the second, we set $f(u) = \frac{1}{2}\text{Sign}(u)u^2$ to obtain the second restoration. The following parameters were used for both experiments: $\varepsilon = 4$, $r = 0.8$, $F(u, v) = \text{Sign}(u)\text{Sign}(v)$ and $a \equiv 1$. We observe that in both cases, the signal is perfectly restored. Furthermore, we remark the influence of the propagation velocity control through the function $f(u)$ on the restoration process. The restoration required 10 iterations for the first choice of f, while the second choice achieved the same result in only four iterations. The choice of ($f(u) = \frac{1}{2}\text{Sign}(u)u^2$) favours the creation of discontinuities (shocks) near the zones where the function's value approaches ± 1. This makes the process faster than the first choice, as shown in the figure.

10.2. Two-Dimensional Case (Images)

Figure 2 presents the acceleration process of convergence on the two-dimensional case by a smart choice of

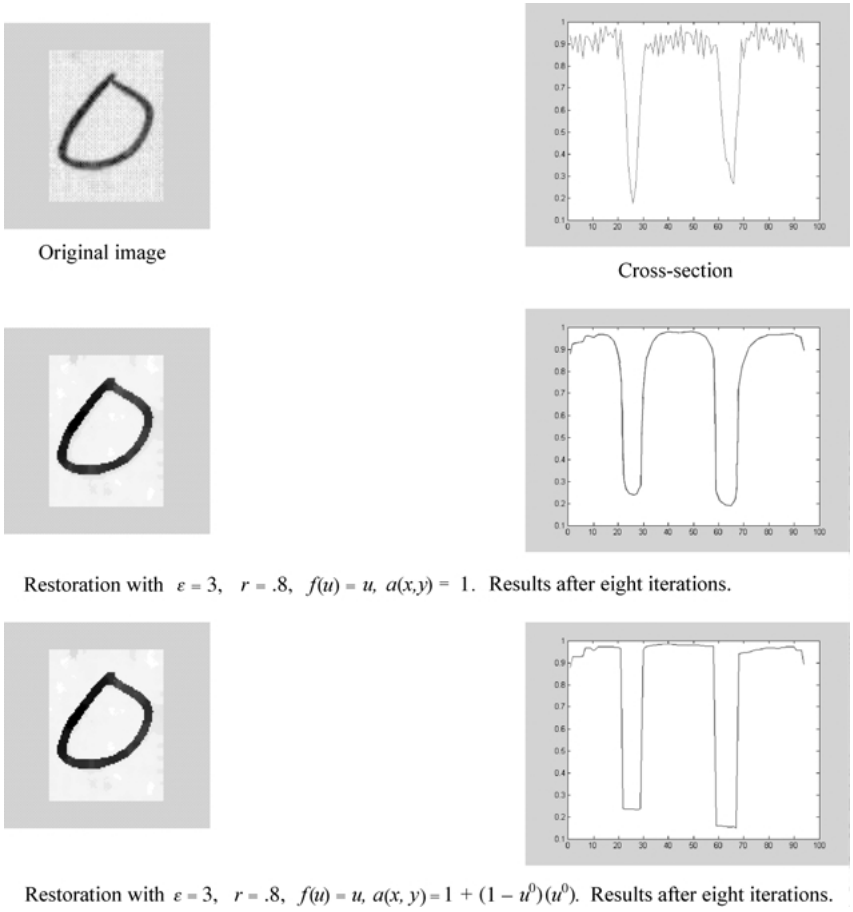

Figure 3. Handwritten data test case. Convergence speed using different values of the coefficient $a(x)$ for handwritten real data images.

(*Continued on next page*.)

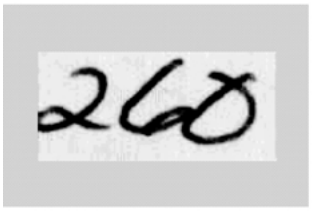

Original image

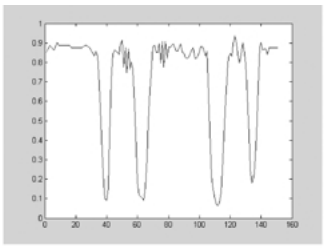

Cross-section

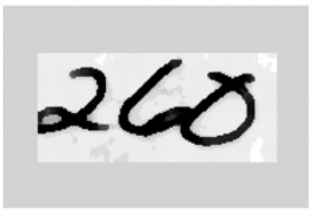

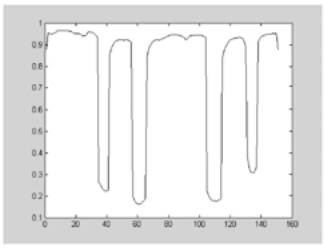

Restoration with $\varepsilon = 3,\ r = .8,\ f(u) = u,\ a(x,y) = 1$. Results after eight iterations.

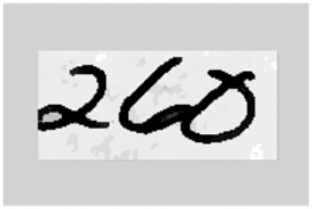

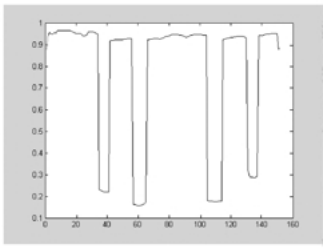

Restoration with $\varepsilon = 3,\ r = .8,\ f(u) = u,\ a(x,y) = 1 + (1 - u^0)(u^0)$. Results after eight iterations.

Figure 3. (*Continued*).

the coefficient $a(x)$. More specifically, we set $a(x, y) = 1+(1-u^0)(1+u^0)$; this choice is motivated by the fact that the two-dimensional curve reaches its extremum at 1 and -1. Consequently, we accelerate the shock's velocity while we are far from the extremum, and the coefficient tends to 1 in the neighbourhood of the extremum to globally respect the CFL condition. The steady state of the model is taken as the restored image, and the quantity $R^n = \sum_{i,j\in Z} |u_{i,j}^{n+1} - u_{i,j}^n|$ is considered as a residual. Figure 2 shows that after seven iterations, the signal is perfectly restored with the last choice of $a(x)$ comparable to the result obtained with $a(x) \equiv 1$. The residuals' curves are also compared, and we can see how the convergence (to the steady state) is accelerated. The accelerator $a(x)$ defined in this test could be generalized to bi-level images (e.g handwritten data images) by taking $a(x) = 1 + (\text{Max} - u^0(x))(u^0(x) - \text{Min})$, where Max and Min are the image's maximum and minimum values. Figure 3 shows tests on handwritten data. These tests show once again the efficiency of the accelerator on the convergence speed. After eight iterations, a clear convergence progress shown by the cross-sections is obtained when the accelerator is used.

Moreover, and for the sake of comparison with other models, Fig. 4 shows the restoration of the handwritten image processed above using the Alvarez-Mazorra model (the numerical scheme proposed by Alvarez et al. is implemented; see [2] for a different parameter signification). Results after 5, 15 and 20 iterations are shown. We note over the cross-sections that after 20 iterations the restored image (the steady state in our definition, the asymptotic state in the Alvarez et al. definition) has not been reached.

In Fig. 5–7, the two-dimensional proposed numerical scheme is applied to a blurred synthetic image (the square and disc image), as well as to a real scene (the pictures of the car, the truck and the painting) with

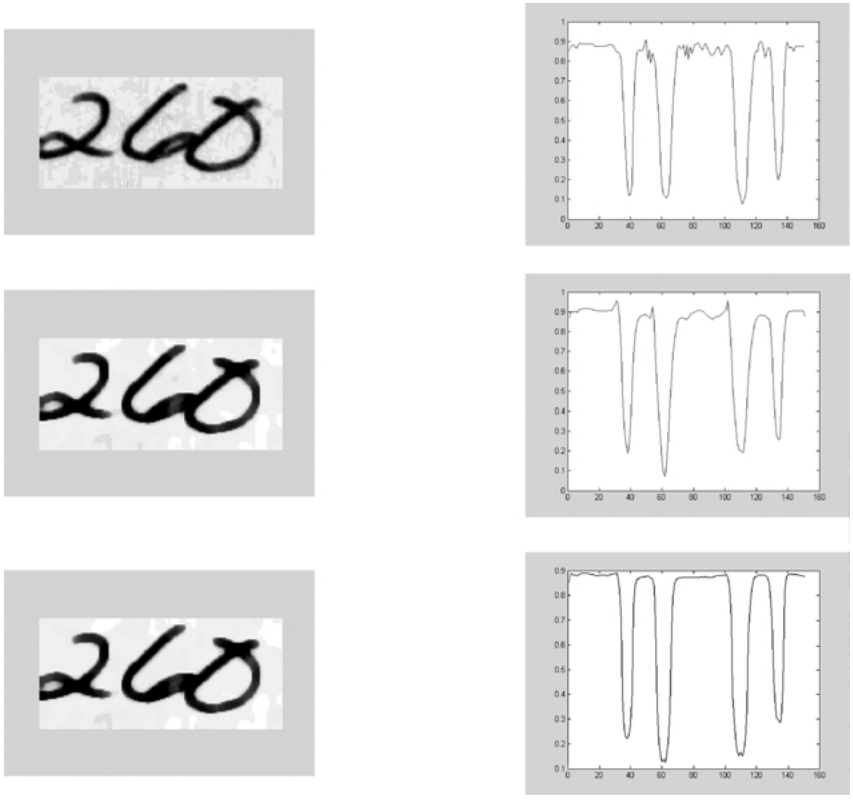

Figure 4. Restoration using the Alvarez and Mazorra model: $\sigma = 3$, time step $= 1$, $C = 1$. Results after 5, 15 and 20 iterations.

parameters given for each. The restoration results for the synthetic image and the enhancement of the real car and painting images are tangible. Note that by interpreting the model within the framework of the generalized function algebra we handle representatives, which are smooth functions. As such, the original signal is smoothed and almost all the noise is removed at the beginning. Moreover, such a model does not use any *a priori* information about the noise.

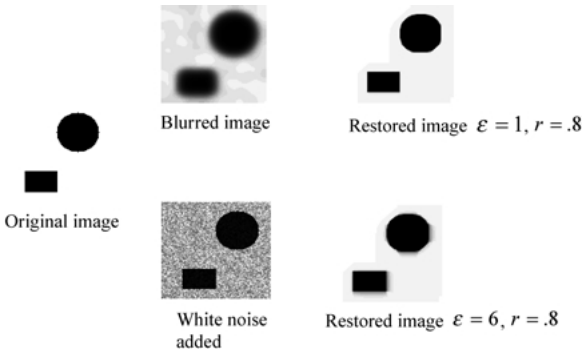

Figure 5. Test on a synthetic image with $a(x, y) = 1 + (1 - u^0)(u^0)$, $f(u) = u$. Results after seven iterations.

Remark. Note that for comparison purposes, the images were normalized before processing in order to keep the same CFL conditions for varying choices of $a(x)$ and $f(u)$.

11. Conclusion

In this paper, we have proposed a generalized one-dimensional shock model for the enhancement and restoration of signals where the shock propagation speed is well controlled. Controlling the propagation speed renders the model more robust and efficient for different applications. We have shown that interpreting the model in a recently-developed framework of the generalized function algebra makes it well-posed, when it is usually ill-posed in the classical theory of

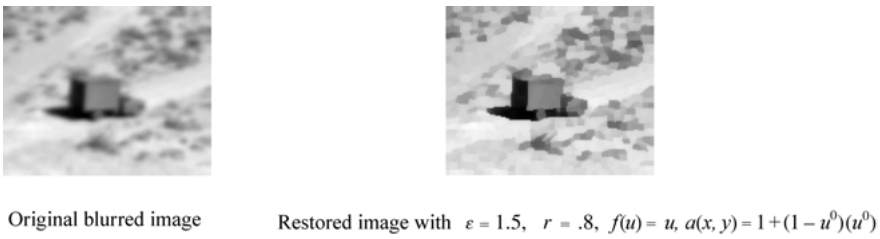

Figure 6. Test on blurred real scene with real size. Results after seven iterations.

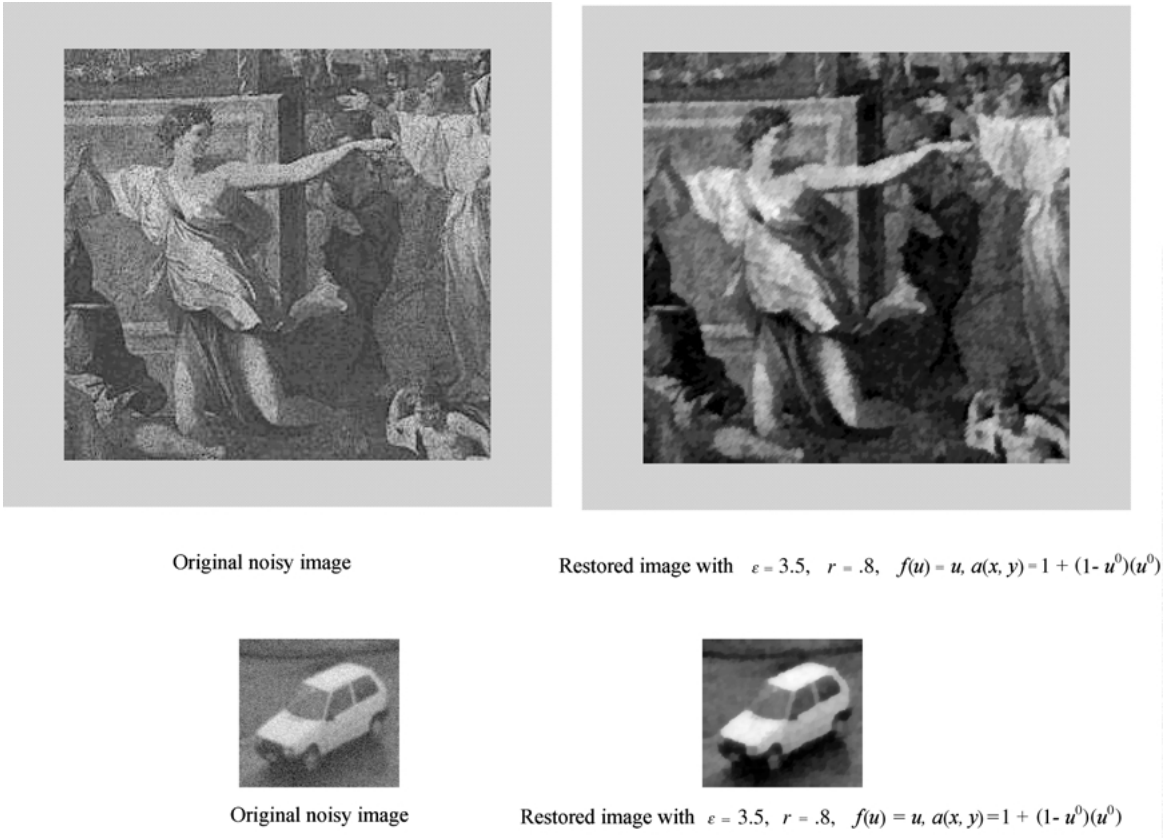

Figure 7. Tests on real scenes with real sizes without added blurring or noise. Results after seven iterations.

distributions because of the coefficients' discontinuity. An efficient numerical scheme for one-dimensional signals is obtained from the discretization of the proposed continuous model. Using a space-split strategy, we derived a numerical scheme for two-dimensional signals (images) from the one-dimensional model. A stability result for both schemes was proved. High-quality results showing the enhancement and restoration performance of the derived schemes, as well as the influence of the shock speed control on the processing time, are also presented.

Appendix

Proof of the Proposition

The One-Dimensional Case

First set

$$\alpha_i^n = \mathrm{Max}\left[0, a_i F\left(\frac{u_{i+1}^{0,\varepsilon} - 2u_i^{0,\varepsilon} + u_{i-1}^{0,\varepsilon}}{h^2}, \frac{u_i^{0,\varepsilon} - u_{i-1}^{0,\varepsilon}}{h}\right) f'\left(u_i^{\varepsilon,n}\right)\right]$$

and

$$\beta_i = \mathrm{Min}\left[0, a_i F\left(\frac{u_{i+1}^{0,\varepsilon} - 2u_i^{0,\varepsilon} + u_{i-1}^{0,\varepsilon}}{h^2}, \frac{u_{i+1}^{0,\varepsilon} - u_i^{0,n}}{h}\right) f'\left(u_i^{\varepsilon,n}\right)\right]$$

The numerical scheme is then rewritten

$$u_i^{\varepsilon,n+1} = u_i^n - r\alpha_i^n\left(u_i^{\varepsilon,n} - u_{i-1}^{\varepsilon,n}\right) - r\beta_i^n\left(u_{i+1}^{\varepsilon,n} - u_i^{\varepsilon,n}\right) \tag{8}$$

Using the CFL condition $\|raFf'\| < \frac{1}{2}$, we have

$$\alpha_i^n \geq 0 \quad \text{and} \quad \left|r\alpha_i^n\right| \leq \frac{1}{2} \tag{9}$$

$$\beta_i^n \leq 0 \quad \text{and} \quad \left|r\beta_i^n\right| \leq \frac{1}{2}. \tag{10}$$

Proof of (i): From (8) we have:

$$u_i^{\varepsilon,n+1} = \left(1 - \alpha_i^n + r\beta_i^n\right)u_i^n + r\alpha_i^n u_{i-1}^{\varepsilon,n} - r\beta_i^n u_{i+1}^{\varepsilon,n}$$

by taking (8) and (9) into account, we achieve:

$$\begin{aligned}
&\left|u_i^{\varepsilon,n+1}\right| \\
&\quad \leq \left(1 - \alpha_i^n + r\beta_i^n\right)\left|u_i^n\right| + r\alpha_i^n\left|u_{i-1}^{\varepsilon,n}\right| \\
&\qquad - r\beta_i^n\left|u_{i+1}^{\varepsilon,n}\right| \leq \left(1 - \alpha_i^n + r\beta_i^n\right)\operatorname*{Sup}_{i\in IZ}\left|u_i^{\varepsilon,n}\right| \\
&\qquad + r\alpha_i^n \operatorname*{Sup}_{i\in IZ}\left|u_{i-1}^{\varepsilon,n}\right| - r\beta_i^n \operatorname*{Sup}_{i\in IZ}\left|u_{i+1}^{\varepsilon,n}\right| = \operatorname*{Sup}_{i\in IZ}|u_i^{\varepsilon,n}|
\end{aligned}$$

Then, recursively, we obtain:

$$\left|u_i^{\varepsilon,n+1}\right| \leq \operatorname*{Sup}_i u_i^{\varepsilon,0} \leq \|u_0\|_{L^\infty(\Re)}$$

□

To prove (ii) and (iii), we first need to prove the following two assertions:

$$(*): \sum_{i\in Z}\left|u_i^{n+1} - u_i^n\right| \leq \sum_{i\in Z}\left|u_{i+1}^n - u_i^n\right|$$

$$(**): \sum_{i\in Z}\left|u_{i+1}^{n+1} - u_i^{n+1}\right| \leq \sum_{i\in Z}\left|u_{i+1}^n - u_i^n\right|$$

As such, (ii) is obtained recursively from $(**)$, and (iii) is obtained by combining $(*)$ and $(**)$ in a recursive fashion.

Proof of (*): From (7), we have the inequality

$$\left|u_i^{\varepsilon,n+1} - u_i^{\varepsilon,n}\right| \leq \alpha_i^n r\left|u_i^{\varepsilon,n} - u_{i-1}^{\varepsilon,n}\right| + r\left|\beta_i^n\right|\left|u_{i+1}^{\varepsilon,n} - u_i^{\varepsilon,n}\right|$$

Using (8) and (9) once again, we obtain

$$\left|u_i^{\varepsilon,n+1} - u_i^{\varepsilon,n}\right| \leq \frac{1}{2}\left|u_i^{\varepsilon,n} - u_{i-1}^{\varepsilon,n}\right| + \frac{1}{2}\left|u_{i+1}^{\varepsilon,n} - u_i^{\varepsilon,n}\right|$$

The two quantities on the right are the same up to a shift of index i. By summing over the index i we obtain $(*)$, specifically:

$$\sum_{i\in IZ}\left|u_i^{\varepsilon,n+1} - u_i^{\varepsilon,n}\right| \leq \sum_{i\in IZ}\left|u_{i+1}^{\varepsilon,n} - u_i^{\varepsilon,n}\right|$$

□

Proof of (**): Let us express (7) at i and $i+1$

$$\begin{aligned}
u_i^{\varepsilon,n+1} &= u_i^n - r\alpha_i^n\left(u_i^{\varepsilon,n} - u_{i-1}^{\varepsilon,n}\right) - r\beta_i^n\left(u_{i+1}^{\varepsilon,n} - u_i^{\varepsilon,n}\right) \\
u_{i+1}^{\varepsilon,n+1} &= u_{i+1}^n - r\alpha_{i+1}^n\left(u_{i+1}^{\varepsilon,n} - u_i^{\varepsilon,n}\right) \\
&\quad - r\beta_{i+1}^n\left(u_{i+2}^{\varepsilon,n} - u_{i+1}^{\varepsilon,n}\right)
\end{aligned}$$

We have:

$$\begin{aligned}
&u_{i+1}^{n+1} - u_i^{n+1} \\
&\quad = \left(1 + r\beta_1^n - r\alpha_{i+1}^n\right)\left(u_{i+1}^n - u_i^n\right) \\
&\qquad + r\alpha_i^n\left(u_i^n - u_{i-1}^n\right) - r\beta_{i+1}^n\left(u_{i+2}^n - u_{i+1}^n\right)
\end{aligned}$$

Taking (8) and (9) into account, we obtain:

$$\begin{aligned}
&\left|u_{i+1}^{n+1} - u_i^{n+1}\right| \\
&\quad \leq \left(1 + r\beta_i^n - r\alpha_{i+1}^n\right)\left|u_{i+1}^n - u_i^n\right| \\
&\qquad + r\alpha_i^n\left|u_i^n - u_{i-1}^n\right| - r\beta_{i+1}^n\left|u_{i+2}^n - u_{i+1}^n\right|
\end{aligned}$$

Summing over index i

$$\begin{aligned}
&\sum_{i\in Z}\left|u_{i+1}^{n+1} - u_i^{n+1}\right| \\
&\quad \leq \sum_{i\in Z}\left(1 + r\beta_i^n - r\alpha_{i+1}^n\right)\left|u_{i+1}^n - u_i^n\right| \\
&\qquad + \sum_{i\in Z} r\alpha_i^n\left|u_i^n - u_{i-1}^n\right| - \sum_{i\in Z} r\beta_{i+1}^n\left|u_{i+2}^n - u_{i+1}^n\right|
\end{aligned}$$

By shifting the index i forward and back in the last two quantities, we achieve:

$$\sum_{i\in Z}\left|u_{i+1}^{n+1}-u_i^{n+1}\right| \leq \sum_{i\in Z}\left(1+r\beta_i^n-r\alpha_{i+1}^n\right)\left|u_{i+1}^n-u_i^n\right| + \sum_{i\in Z} r\alpha_{i+1}^n\left|u_{i+1}^n-u_i^n\right| - \sum_{i\in Z} r\beta_i^n\left|u_{i+1}^n-u_i^n\right|$$

Which finally gives us:

$$\sum_{i\in Z}\left|u_{i+1}^{n+1}-u_i^{n+1}\right| \leq \sum_{i\in Z}\left|u_{i+1}^n-u_i^n\right|$$

□

The Two-Dimensional Case

Proof of (i): Following the same method as for the proof of the one-dimensional case, we show from (5) that

$$\left|u_{i,j}^{\varepsilon,n+\frac{1}{2}}\right| \leq \operatorname*{Sup}_{i,j\in IZ}\left|u_{i,j}^{\varepsilon,n}\right|$$

and from (6) that

$$\left|u_{i,j}^{\varepsilon,n+1}\right| \leq \operatorname*{Sup}_{i,j\in IZ}\left|u_{i,j}^{\varepsilon,n+\frac{1}{2}}\right|$$

This achieves the proof of (i). □

Proof of (ii) and (iii): Similarly, and by using the same steps as in Proposition 1, we prove that:

$$(^*1):\ \sum_{i,j\in Z}\left|u_{i,j}^{n+\frac{1}{2}}-u_{i,j}^n\right| \leq \sum_{i,j\in Z}\left|u_{i+1,j}^n-u_{i,j}^n\right|$$

$$(^*2):\ \sum_{i,j\in Z}\left|u_{i,j}^{n+1}-u_{i,j}^{n+\frac{1}{2}}\right| \leq \sum_{i,j\in Z}\left|u_{i,j+1}^{n+\frac{1}{2}}-u_{i,j}^{n+\frac{1}{2}}\right|$$

$$(^*3):\ \sum_{i,j\in Z}\left|u_{i+1,j}^{n+\frac{1}{2}}-u_{i,j}^{n+\frac{1}{2}}\right| \leq \sum_{i,j\in Z}\left|u_{i+1,j}^n-u_{i,j}^n\right|$$

$$(^*4):\ \sum_{i,j\in Z}\left|u_{i,j+1}^{n+1}-u_{i,j}^{n+1}\right| \leq \sum_{i,j\in Z}\left|u_{i,j+1}^{n+\frac{1}{2}}-u_{i,j}^{n+\frac{1}{2}}\right|$$

$$(^*5):\ \sum_{i,j\in Z}\left|u_{i,j+1}^{n+\frac{1}{2}}-u_{i,j}^{n+\frac{1}{2}}\right| \leq \sum_{i,j\in Z}\left|u_{i,j+1}^n-u_{i,j}^n\right|$$

$$(^*6):\ \sum_{i,j\in Z}\left|u_{i+1,j}^{n+1}-u_{i,j}^{n+1}\right| \leq \sum_{i,j\in Z}\left|u_{i+1,j}^{n+\frac{1}{2}}-u_{i,j}^{n+\frac{1}{2}}\right|$$

From (*6) and (*4), we have:

$$\sum_{i,j\in Z}\left|u_{i+1,j}^{n+1}-u_{i,j}^{n+1}\right|+u_{i,j+1}^{n+1}-u_{i,j}^{n+1}\Big| \leq \sum_{i,j\in Z}\left|u_{i+1,j}^{n+\frac{1}{2}}-u_{i,j}^{n+\frac{1}{2}}\right| + \sum_{i,j\in Z}\left|u_{i,j+1}^{n+\frac{1}{2}}-u_{i,j}^{n+\frac{1}{2}}\right|$$

Combining (*3) and (*5), we obtain

$$\sum_{i,j\in Z}\left|u_{i+1,j}^{n+1}-u_{i,j}^{n+1}\right|+u_{i,j+1}^{n+1}-u_{i,j}^{n+1}\Big| \leq \sum_{i,j\in Z}\left|u_{i+1,j}^n-u_{i,j}^n\right|+u_{i,j+1}^n-u_{i,j}^n\Big|$$

Recursively, we achieve (ii).

To prove (iii), break down $\sum_{i,j\in Z}|u_{i,j}^{n+1}-u_{i,j}^n|$ as follows

$$\sum_{i,j\in Z}\left|u_{i,j}^{n+1}-u_{i,j}^n\right| \leq \sum_{i,j\in Z}\left|u_{i,j}^{n+1}-u_{i,j}^{n+\frac{1}{2}}\right|+\left|u_{i,j}^{n+\frac{1}{2}}-u_{i,j}^n\right|$$

Using (*1) and (*2), we obtain:

$$\sum_{i,j\in Z}\left|u_{i,j}^{n+1}-u_{i,j}^n\right| \leq \sum_{i,j\in Z}\left|u_{i,j+1}^{n+\frac{1}{2}}-u_{i,j}^{n+\frac{1}{2}}\right|+\left|u_{i+1,j}^n-u_{i,j}^n\right|$$

And from (*5):

$$\sum_{i,j\in Z}\left|u_{i,j}^{n+1}-u_{i,j}^n\right| \leq \sum_{i,j\in Z}\left|u_{i,j+1}^n-u_{i,j}^n\right|+\left|u_{i+1,j}^n-u_{i,j}^n\right|$$

We conclude by using (ii). □

References

1. L. Alvarez, P.L. Lions, and J.M. Morel, "Image selective smoothing and edge detection by nonlinear diffusion (ii)," *SIAM J. Numer. Anal.*, Vol. 29, No. 3, pp. 845–866, 1992.
2. L. Alvarez and L. Mazorra, "Signal and image restoration using shock filters and anisotropic diffusion," *SIAM J. Num. Anal.*, Vol. 31, No. 2, pp. 590–605, 1994.
3. J.F. Colombeau, "Multiplication of distribution," in *Lecture Notes in Mathematics*, Vol. 1532, Springer-Verlag; Berlin, 1992.
4. J.F. Colombeau and A. Heibig, "Generalized solution to Cauchy problems," in *Mh. Math.*, Vol. 117, Springer-Verlag: Berlin, 1994, pp. 33–49.
5. E. Godlewski and P.A. Raviart, "Hyperbolic systems of conservation laws," *SMAI*, No. 3/4, 1991.
6. J.J. Koenderink, "The Structure of images," *Biological Cybernetics*, Vol. 53, pp. 363–370, 1984.
7. M. Oberguggeenberger, "Hyperbolic systems with discontinuous coefficients: Generalized solutions and transmission problems in acoustic," *J. M. App.*, Vol. 142, 1989.

8. S. Osher and L. Rudin, "Feature oriented image enhancement using shock filters," *SIAM J. Numer. Anal.*, Vol. 27, No. 4, pp. 919–940, 1990.
9. P. Perona and J. Malik, "Scale-space and edge detection using anisotropic diffusion," *IEEE Trans. On Patt. Anal. and Mach Int.*, Vol. 12, No. 7, pp. 629–639, 1990.
10. L. Remaki, "Étude théorique et numérique des équations quasi-linéaires à coefficients discontinus et acoustique linéaire 2D," Ph.D. Thesis, Claude Bernard University, Lyon, France, 1997.
11. L. Remaki and M. Cheriet, "KCS—New Kernel family with compact support in scale space: Formulation & impact," *IEEE Transaction on Image Processing*, Vol. 9, No. 6, p. 970, 2000.

Remaki Lakhdar received his B.S. degree in mathematics from Université des Sciences et Technologie d'Alger (Bab Ezzouar, Algiers, Algeria) in 1991, and received the M.Sc. and Ph.D. degrees in applied mathematics from Université Claude Bernard de Lyon (France) in 1992 and 1997 respectively. From 1998 to 2001, he was a postdoctoral fellow at the École de Technologie Supérieure de l'Université du Québec à Montréal, É.T.S. Since 2001 he is a research associate at McGill university.

His research interest include mathematical modeling for image process, partial differential equations and numerical analysis and their application to both signal analysis and computational fluid dynamic.

Mohamed Cheriet received his B. Eng. degree in computer science from Université des Sciences et de Technologie d'Alger (Algiers) in 1984, and received his M.Sc. and Ph.D. degrees, also in computer science, from University of Pierre et Marie Curie (Paris VI) in 1985 and 1988, respectively. Dr. Cheriet was appointed Assistant Professor in 1992, Associate Professor in 1995, and Full Professor in 1998 in the Department of Automation Engineering, École de technologie superieure (ETS) of University of Quebec, in Montreal. Currently, he is the Director of LIVIA, the Laboratory for Imagery, Vision and Artificial Intelligence at ETS, and an active member of CENPARMI, the Centre for Pattern Recognition and Machine Intelligence. Prof. Cheriet's research focuses on mathematical modeling for signal and image processing, pattern recognition, character recognition, text processing, documents analysis and recognition, and perception. He has published more than 90 technical papers in the field. He was a guest editor of the International Journal of Pattern Recognition and Artificial Intelligence and the Machine, Perception, and Artificial Intelligence series books, published by World Scientific. He was the Co-Chair of the 11th and the 13th Vision Interface Conferences held respectively in Vancouver, in 1998 and in Montreal, in 2000. He is currently the General Co-Chair of the 8th International Workshop on Frontiers on Handwriting Recognition, to be held in Niagara-on-the-lake in 2002. Dr. Cheriet is a senior member of IEEE.